



## A terephthalate-bridged two-dimensional heteronuclear Cu(II)–Mn(II) complex with a terminal 2,2'-dipyridylamine ligand

LIDIJA RADOVANOVIC<sup>1\*</sup>, JELENA ROGAN<sup>2#</sup>, DEJAN POLETI<sup>2#</sup>,  
MARKO V. RODIĆ<sup>3</sup> and ZVONKO JAGLIČIĆ<sup>4</sup>

<sup>1</sup>Innovation Center of the Faculty of Technology and Metallurgy, University of Belgrade,  
Karnegijeva 4, 11000 Belgrade, Serbia, <sup>2</sup>Department of General and Inorganic Chemistry,  
Faculty of Technology and Metallurgy, University of Belgrade, Karnegijeva 4, 11000  
Belgrade, Serbia, <sup>3</sup>Faculty of Sciences, University of Novi Sad, Trg Dositeja Obradovića 3,  
21000 Novi Sad, Serbia and <sup>4</sup>Faculty of Civil and Geodetic Engineering & Institute of  
Mathematics, Physics and Mechanics, University of Ljubljana, Jamova 2,  
1000 Ljubljana, Slovenia

(Received 25 April, revised 8 June, accepted 7 July 2017)

**Abstract:** A terephthalate-bridged heteronuclear Cu(II)–Mn(II) complex  $[\text{Cu}_2\text{Mn}(\text{dipy})_2(\text{tpht})_3]_n$ , **I**, where dipy is 2,2'-dipyridylamine and tpht is the anion of 1,4-benzenedicarboxylic (terephthalic,  $\text{H}_2\text{tpht}$ ) acid was synthesized under hydrothermal conditions. The obtained complex **I** was characterized by a single-crystal X-ray diffraction, FTIR spectroscopy, TG/DSC analysis and magnetic measurements. The Cu(II) and Mn(II) metal centers adopt distorted octahedral geometry and they are linked by bridging tpht ligands. Two crystallographically different tpht anions are coordinated as tridentate and hexadentate ligands forming two-dimensional layers. The layers are interconnected by hydrogen bonds and additionally stabilized by non-covalent C–H $\cdots$  $\pi$  interactions. The measurements of magnetic susceptibility proved that **I** is an almost perfect paramagnet.

**Keywords:** heterometallic complex; crystal structure; Cu(II); Mn(II); 1,4-benzenedicarboxylate; magnetic properties.

### INTRODUCTION

During the past decades, heterometallic coordination compounds have achieved great attention due to their possible applications in gas storage, catalysis, magnetism, etc.<sup>1</sup> Metal–organic systems established between two paramagnetic metal centers are especially attractive because they could result in

\* Corresponding author. E-mail: iradovanovic@tmf.bg.ac.rs

# Serbian Chemical Society member.

<https://doi.org/10.2298/JSC170425086R>

many novel compounds with potential application as molecular-based magnetic materials.<sup>2</sup> The advantageous strategy to obtain such structures is to use adequate bridging ligands that can form coordination bonds with metal ions, which further eventually lead to the appearance of magnetic interactions.<sup>3</sup> The anions of the three positional isomers of benzenedicarboxylic ( $H_2BDC$ ) acids have been shown to be the most potent candidates for this purpose. Despite the fact that magnetic interactions over  $BDC^{2-}$  bridges are not so strong,<sup>4</sup> the intensity and character of the magnetic interactions can be controlled by several factors, such as the distance between the metal centers,<sup>5</sup> coordination mode of the  $BDC^{2-}$  anions,<sup>6</sup> dihedral angle between the equatorial plane of the transition metal (TM) and the anion, and the dihedral angles between the planes of the COO groups and the aromatic ring.<sup>7</sup> Magnetic interactions in TM complexes with the dianion of terephthalic ( $H_2tpht$ ) acid as bridge between paramagnetic metal ions have been widely investigated,<sup>8</sup> in contrast to those with the anions of isophthalic and phthalic acids. This was, probably, due to the fact that magnetic interactions over the bridging ligand were originally observed in tpht complexes in which the separation among metal centers was about 11 Å.<sup>9–14</sup>

The tpht dianion has been promoted to construct an enormous number of fascinating supramolecular architectures for two main reasons: a) it can be coordinated to the metal ions in different modes ranging from monodentate to octadentate<sup>8,15</sup> and b) it can participate in the formation of non-covalent interactions, such as hydrogen bonding and/or  $\pi$ – $\pi$  overlapping interactions.<sup>16–19</sup> Finding crystal structures with diverse coordination modes of tpht anion within the same structure is not uncommon and many examples have already been reported (see for example references<sup>19,20</sup>).

In the present paper, the synthesis, crystal structure, spectroscopic, thermal and magnetic properties of the heteronuclear Cu(II)–Mn(II) complex  $[Cu_2Mn(dipy)_2(tpht)_3]_n$ , **I**, where dipya corresponds to 2,2'-dipyridylamine, are reported. According to the search of CSD,<sup>21</sup> there are about 270 bimetallic Cu–Mn complexes and among them, there is only one compound that contains simultaneously  $Cu^{2+}$ ,  $Mn^{2+}$  and tpht<sup>2-</sup>,<sup>22</sup> but with dissimilar terminal ligands. Regarding the nature of the Cu(II) and Mn(II) ions, as well as the number and symmetry of their magnetic orbitals (one per Cu(II) in contrast to five per Mn(II) ion), significant magnetic interactions between them could be expected.

## EXPERIMENTAL

### Materials and measurements

Except dipya, which was of *purum* quality, all reagents were of analytical grade and used without further purification. The FTIR spectra were recorded on a Bomem MB-100, Hartmann Braun FTIR spectrophotometer (4000–400  $cm^{-1}$  region) in KBr pellets. The thermal properties of the complex were examined from room temperature up to 850 °C on an SDT Q600 TGA/DSC instrument (TA Instruments). The heating rate was 20 °C  $min^{-1}$  using a

sample mass of less than 10 mg. The furnace atmosphere consisted of dry nitrogen at a flow rate of  $100 \text{ cm}^3 \text{ min}^{-1}$ . Magnetic measurements were recorded on a Quantum Design MPMS XL-5 SQUID magnetometer equipped with a 5 T magnet.

*Synthesis and crystallization*

The reaction mixture of 1 M  $\text{Mn}(\text{NO}_3)_2$  ( $0.1 \text{ cm}^3$ , 0.1 mmol), 1 M  $\text{Cu}(\text{NO}_3)_2$  ( $0.1 \text{ cm}^3$ , 0.1 mmol), dipya ( $0.0342 \text{ g}$ , 0.2 mmol), 0.2 M  $\text{Na}_2\text{tpht}$  ( $1.0 \text{ cm}^3$ , 0.2 mmol) and  $\text{H}_2\text{O}$  ( $3 \text{ cm}^3$ ) was placed in a Teflon-lined steel autoclave, heated at  $160^\circ\text{C}$  for 4 days and cooled for 8 h to room temperature. Green single crystals, insoluble in water, ethanol and DMSO, were obtained. Yield: 35 %; FTIR (KBr pellet,  $\text{cm}^{-1}$ ):  $3443\text{br}$  (N–H),  $1653\text{s}$  (C=N),  $1580\text{s}$  (COO),  $1477\text{s}$  (C=C, C=N),  $1375\text{s}$  (COO),  $743\text{s}$  (N–H).

*X-ray structure determination*

Single-crystal X-ray diffraction data were collected at room temperature ( $298 \text{ K}$ ) on an Oxford Gemini S diffractometer equipped with CCD detector using monochromatized  $\text{MoK}\alpha$  radiation ( $\lambda = 0.71073 \text{ \AA}$ ). Intensities were corrected for absorption using the multi-scan method. The structure was solved by direct methods (SIR2014)<sup>23</sup> and refined on  $F^2$  by full-matrix least-squares using the programs SHELXL-2014/7<sup>24</sup> and WinGX.<sup>25</sup> All non-hydrogen atoms were refined anisotropically. The positions of the H atoms connected to C atoms were calculated on geometric criteria and refined using the riding model with  $U_{\text{iso}} = 1.2U_{\text{eq}}(\text{C})$ . Hydrogen atom bonded to N3 was found in  $\Delta F$  maps and added to the structural models before the final cycle of refinement. Selected crystal data, data collection and refinement results for **I** are listed in Table I.

TABLE I. Crystal data, data collection and structure refinement for **I**;  $w = 1 / [s^2(F_o^2) + + (0.0306P)^2 + 3.9555P]$ , where  $P = (F_o^2 + 2F_c^2)/3$

Crystal data	Value	Data collection
Chemical formula	$\text{C}_{44}\text{H}_{30}\text{Cu}_2\text{MnN}_6\text{O}_{12}$	$T_{\min}, T_{\max}$ 0.93643, 1.00000
$M_r$	1016.78	$F(000)$ 2060
Crystal system	Orthorhombic	$\theta$ range, ° 3.06–26.02
Space group	$Pbca$	Limiting indices $-13 \leq h \leq 13$
$a / \text{\AA}$	10.901(2)	$-19 \leq k \leq 19$
$b / \text{\AA}$	16.032(3)	$-29 \leq l \leq 29$
$c / \text{\AA}$	23.843(5)	Measured reflections 31134
$V / \text{\AA}^3$	4166.9(14)	Independent reflections 4096
$Z$	4	Reflections with $I > 2\sigma(I)$ 3729
$\mu / \text{mm}^{-1}$	1.383	$R_{\text{int}}$ 0.0253
Crystal size, mm <sup>3</sup>	0.41×0.21×0.15	Refinement
$\rho_c / \text{g cm}^{-3}$	1.621	$R$ indices [ $I > 2\sigma(I)$ ] $R_1 = 0.0269$ , $wR_2 = 0.0683$
		$R$ indices (all data) $R_1 = 0.0305$ , $wR_2 = 0.0702$
		No. of restraints 0
		No. of parameters 299
		Goodness-of-fit 1.049
		$\Delta\rho_{\text{max}}, \Delta\rho_{\text{min}} / \text{e \AA}^{-3}$ 0.355, -0.430

## RESULTS AND DISCUSSION

*Description of the crystal structure of I*

Single-crystal X-ray diffraction reveals that complex **I** crystallizes in the orthorhombic space group *Pbca* and exhibits a two-dimensional structure. The structural fragment consists of two Cu(II) cations, one Mn(II) cation in the centre of the symmetry, two dipya ligands and three tpht<sup>2-</sup> (Fig. 1).

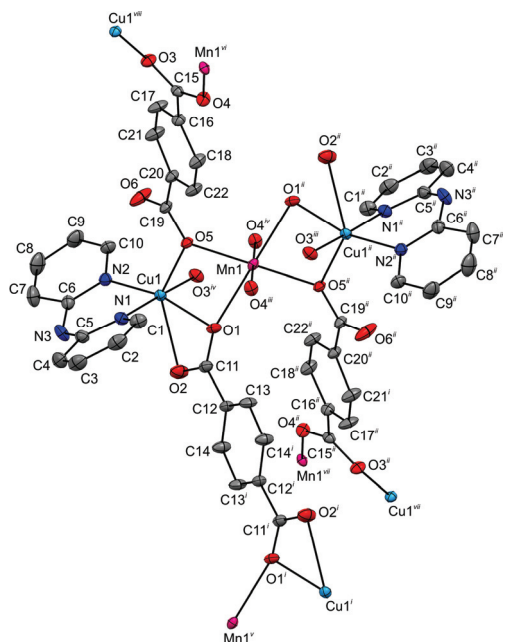


Fig 1. The structural fragment of **I**. The H atoms are omitted for sake of clarity. Ellipsoids were drawn at the 30 % probability level. Symmetry codes: *i*):  $-x+1, -y, -z+1$ ; *ii*):  $-x, -y, -z+1$ ; *iii*):  $x+1/2, -y-1/2, -z+1$ ; *iv*):  $-x-1/2, y+1/2, z$ ; *v*):  $x+1, y, z$ ; *vi*):  $x-1/2, -y-1/2, -z+1$ ; *vii*):  $x+1/2, -y+1/2, -z+1$ ; *viii*):  $-x-1/2, y-1/2, z$ .

The Mn1 cation is located in a slightly deformed octahedral environment with six O atoms (O1, O5, O1<sup>ii</sup>, O4<sup>iii</sup>, O4<sup>iv</sup>, O5<sup>ii</sup>; *ii*):  $-x, -y, -z+1$ ; *iii*):  $x+1/2, -y-1/2, -z+1$ ; *iv*):  $-x-1/2, y+1/2, z$ ) from six different tphts (Table II, Fig. 2). The Mn1–O bond lengths are in the range 2.1094(13)–2.3309(14) Å which are comparable to the bond lengths found in some previously reported Mn(II)–tpht complexes.<sup>16</sup> The Cu1 cation is also six-coordinated, but it adopts a strongly distorted 4+2 octahedral geometry. The two O atoms (O1 and O3<sup>iv</sup>) from two tpht ions and two N atoms (N1 and N2) from dipya exist in the equatorial plane, while the apical positions are occupied by O2 and O5 atoms from two tpht ions (Table II, Fig. 2). The distances between Cu1 and apical atoms (2.4747(17) Å for Cu1–O2 and 2.2810(13) Å for Cu1–O5) are longer than those in the Cu1 equatorial plane due to the Jahn–Teller effect. Among TM complexes, Jahn–Teller elongation is mostly found in Cu(II) coordination compounds and its existence could affect the physical properties of the complexes, such as, for example, magnetism.<sup>26</sup> Furthermore, the small O1–Cu1–O2 angle (57.01(5) $^\circ$ ), as a consequence of chelation

of the C<sub>11</sub>O<sub>1</sub>O<sub>2</sub> group, additionally contributed to the large deformation of the Cu1 octahedron. The Cu1 atom deviates from the planarity of the equatorial plane by 0.0234(3) Å, while the Mn1 atom is coplanar with other atoms in the basal plane. Bond-valence analysis<sup>27</sup> reported satisfactory sum values of 2.09 and 2.08 bond valence units for the Cu1 and Mn1 atoms, respectively.

TABLE II. Selected bond lengths and angles (Å, °) for **I**; symmetry codes: *iii*:  $x+1/2, -y-1/2, -z+1$ ; *iv*:  $-x-1/2, y+1/2, z$

Bond	Bond length, Å	Bonds	Bond angle, °	Bonds	Bond angle, °
O1–Mn1	2.3309(14)	O1–Mn1–O4 <sup>iii</sup>	94.33(5)	N2–Cu1–O2	106.78(6)
O4 <sup>iii</sup> –Mn1	2.1408(15)	O1–Mn1–O5	77.46(5)	N2–Cu1–O3 <sup>iv</sup>	88.89(6)
O5–Mn1	2.1094(13)	O4 <sup>iii</sup> –Mn1–O5	87.89(5)	N2–Cu1–O5	116.96(6)
N1–Cu1	2.0120(17)	N1–Cu1–N2	88.87(7)	O1–Cu1–O2	57.01(5)
N2–Cu1	2.0300(18)	N1–Cu1–O1	89.96(6)	O1–Cu1–O3 <sup>iv</sup>	91.18(6)
O1–Cu1	2.0787(15)	N1–Cu1–O2	88.60(7)	O1–Cu1–O5	79.20(5)
O2–Cu1	2.4747(17)	N1–Cu1–O3 <sup>iv</sup>	175.77(6)	O2–Cu1–O3 <sup>iv</sup>	88.61(6)
O3 <sup>iv</sup> –Cu1	1.9582(14)	N1–Cu1–O5	89.37(6)	O2–Cu1–O5	136.15(5)
O5–Cu1	2.2810(13)	N2–Cu1–O1	163.77(7)	O3 <sup>iv</sup> –Cu1–O5	94.84(5)

The Mn1 polyhedron is linked with two Cu1 polyhedra by sharing edges through common O1 and O5 atoms, causing the formation of the Cu<sub>1</sub>O<sub>1</sub>O<sub>5</sub>Mn1 four-membered ring with an Mn1···Cu1 distance of 3.2504(7) Å. Within the ring, the Cu1–O1 and Mn1–O5 bond lengths are shorter than the other two bonds (Table II), while the Cu1–O1–Mn1 and Cu1–O5–Mn1 angles are almost the same with values of 94.80(6) and 95.44(5)°, respectively. The dihedral angle between the O1O2O5N2 plane of the Cu1 octahedron and the equatorial plane of Mn1 octahedron is 35.30(3)° and these two octahedra are inclined toward each other (Fig. 2). A similar triplet of octahedra was found in complex [Cu<sub>3</sub>(bipym)(tpht)<sub>2</sub>(OH)<sub>2</sub>(H<sub>2</sub>O)<sub>4</sub>]·4H<sub>2</sub>O (bipym = 2,2'-bipyrimidine)<sup>17</sup> in which two crystallographically diverse Cu(II) atoms were found with the angle between their equatorial planes being 67.14 (5)°.

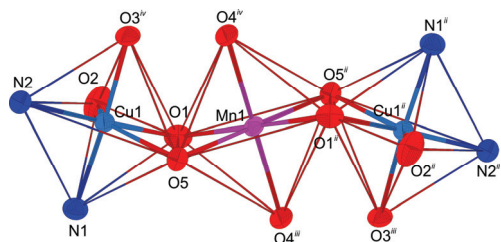


Fig. 2. The coordination octahedra around Cu(II) and Mn(II) cations sharing O1–O5 edges. Symmetry codes: *ii*:  $-x, -y, -z+1$ ; *iii*:  $x+1/2, -y-1/2, -z+1$ ; *iv*:  $-x-1/2, y+1/2, z$ .

The crystal structure of **I** contains two crystallographically different tpht ions, each with a multidentate bridging fashion. Centrosymmetric tpht anion bridges two Cu1 cations as a bis-chelate ligand through C<sub>11</sub>O<sub>1</sub>O<sub>2</sub> groups. Furthermore, this tpht also links two Mn1 cations as a bis-monobridge ligand. The

other tpht ligand bridges one Cu1 and one Mn1 cation with bidentate C15O<sub>3</sub>O<sub>4</sub> group, while in another C19O<sub>5</sub>O<sub>6</sub> group O5 connects both Mn1 and Cu1 cations in a monobridge fashion mode, whereas O6 atom remains uncoordinated. In this way, tpht<sup>2-</sup> in **I** are tridentate and hexadentate. Tridentate coordination mode of COO groups is not so rare and it is found in about 100 TM–tpht complexes.<sup>21</sup> On the contrary, the hexadentate tpht ligand which connects four metal centers, as a combination of one chelate and one monobridging COO group has not hitherto been reported. Therefore, complex **I** could be considered as unique and unprecedented.

Due to the complex coordination modes of the tpht ions, polymeric layers parallel to the *ac*-plane were formed (Fig. 3a). The crystal packing could also be described as triplets of Cu1–Mn1–Cu1 polyhedra cross-linked with different tpht bridges. In the only known structurally characterized Mn–Cu–tpht complex, [CuLMn(tpht)(H<sub>2</sub>O)], where HL is 7,8,15,18-tetrahydro-5,10-dimethylbenzo-[e,m][1,4,8,11]-tetraazacyclotetradecine-16,17-dione, tpht is coordinated as a simple bis-chelate ligand connecting only two Mn(II) cations giving zigzag chains extending along the *c*-axis.<sup>22</sup> The dihedral angle formed between the planes of the carboxylate C11O<sub>1</sub>O<sub>2</sub> group and C12–C14 phenyl ring in **I** is 13.3°, while the angles between C15O<sub>3</sub>O<sub>4</sub> and C19O<sub>5</sub>O<sub>6</sub> and corresponding aromatic ring have the values of 19.5 and 11.0°, respectively, meaning that the tpht ligands deviate from planarity. According to a quantum mechanical study of BDC ligands,<sup>16</sup> planarity is one of the characteristics of tpht dianion, although slight deviations are observed in real systems (see for example reference<sup>12</sup>) as in the case of complex **I**. The metal–metal separation over the tpht bridges ranges from about 9.7 to about 11.3 Å, which well matches the distances found in similar TM–tpht complexes.<sup>16–19</sup> In **I**, dipya is coordinated as usual as a chelate ligand and it is bonded only to the Cu(II) cation. The dihedral angle between the

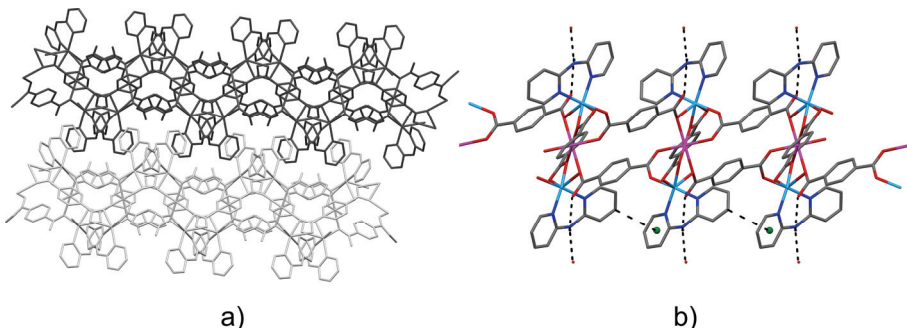


Fig 3. a) The polymeric layers of **I** in the *ac*-plane. The parallel layers are displayed in different colors (dark and light grey); b) the crystal packing diagram of **I** in the *bc*-plane. The hydrogen bonds and C–H···π interactions are presented with dot and dash lines, respectively.

planes of pyridyl rings has the value of  $24.15(6)^\circ$ . Such a great value of this angle is not uncommon, and similar values of analogous angles were previously reported for some TM-dipy-a-tpht complexes.<sup>16,18,19</sup>

The neighboring layers of **I** are linked by  $\text{N}3-\text{H}3\text{A}\cdots\text{O}6^{ix}$  ( $ix$ :  $x+1/2$ ,  $y$ ,  $-z+1/2$ ) intermolecular hydrogen bonds that involve N3 atom from dipy-a and non-coordinated carboxylate O6 atom from tpht in the adjacent layer (Table III, Fig. 3b). Although the N–H bond distance is short with a value of  $0.738(7)$  Å, the hydrogen bond angle is quite regular and amounts  $176(3)^\circ$ . Each layer in **I** is comprised of the hydrophilic and the hydrophobic parts. The hydrogen bonds are located in the hydrophilic parts, while in the hydrophobic parts, the phenyl rings of tpht and pyridyl rings of dipy-a are concentrated (Fig. 3b). Additional stabilization of the layers is achieved by non-covalent edge-to-face interactions *via* the H3 atom from one pyridyl ring and the plane of the closest pyridyl ring at  $\text{H}3\cdots\text{Cg}$  distances of  $2.830$  Å (Fig. 3b).

TABLE III. Geometry of hydrogen bond for **I**; symmetry code:  $ix$ :  $x+1/2$ ,  $y$ ,  $-z+1/2$

$\text{D}-\text{H}\cdots\text{A}$	$d(\text{D}-\text{H})/\text{\AA}$	$d(\text{D}\cdots\text{A})/\text{\AA}$	$d(\text{H}\cdots\text{A})/\text{\AA}$	$\angle\text{D}-\text{H}\cdots\text{A}/^\circ$
$\text{N}3-\text{H}3\text{A}\cdots\text{O}6^{ix}$	$0.738(7)$	$2.781(3)$	$2.045(7)$	$176(3)$

#### Spectral analysis of complex **I**

The FTIR spectrum of **I** (Fig. 4) exhibits a broad band centered at  $3443\text{ cm}^{-1}$  that is ascribed to the N–H vibrations and confirms the existence of dipy-a ligands.

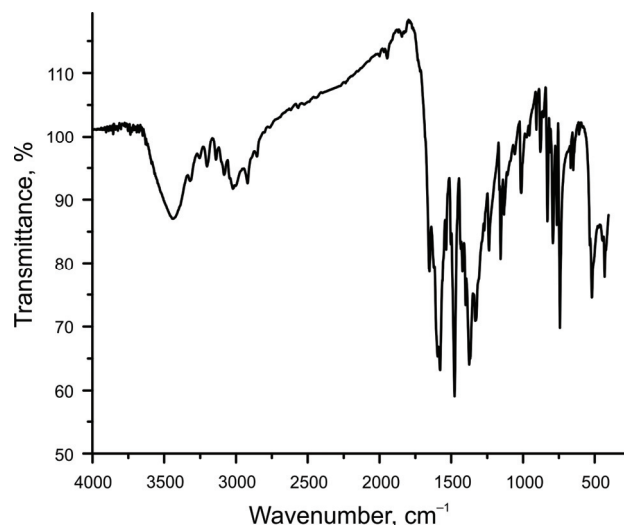


Fig. 4. FTIR spectrum of complex **I**.

The coordinated tpht anions caused the appearance of intense asymmetrical ( $\nu_{as} = 1580\text{ cm}^{-1}$ ) and symmetrical ( $\nu_s = 1375\text{ cm}^{-1}$ ) COO vibrations. A com-

parison of the difference in the values of these two bands ( $\Delta\nu = 205\text{ cm}^{-1}$ ) with the "ionic" value ( $\Delta\nu_l = 173\text{ cm}^{-1}$ ) for  $K_2\text{tpht}^{28}$  suggests monodentate or asymmetric chelate coordination modes of the COO groups,<sup>29,30</sup> which is in accordance with the description of the crystal structure. In the fingerprint region, the strong band at  $743\text{ cm}^{-1}$  is assigned to N–H stretching vibrations and it is probably overlapped with C–H vibrations.<sup>31</sup> A weak band due to Mn–O and Cu–O stretching vibrations located at around  $430\text{ cm}^{-1}$  confirms the coordination of tpht ligands to the central metal atoms.<sup>30</sup>

#### *Thermal properties of complex I*

The TG and DTA curves for **I** are presented in Fig. 5. The thermal decomposition starts at  $230\text{ }^\circ\text{C}$  with the loss of one  $\text{CO}_2$  molecule, which is in very good agreement with the found and calculated mass losses of 4.269 and 4.328 %, respectively.

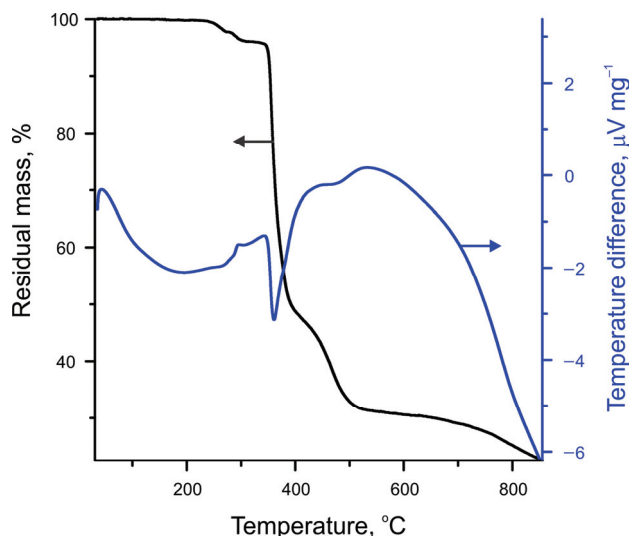


Fig. 5. The TG and DTA curves for **I**.

In addition, up to  $400\text{ }^\circ\text{C}$ , the removal of two  $\text{tpht}^{2-}$  and the residue of the third  $\text{tpht}^{2-}$  was observed (mass loss found: 51.70 %; calcd. 48.42 %). It is quite unusual that decarboxylation occurs in two steps and hitherto, it was not found in the literature. Further degradation up to  $540\text{ }^\circ\text{C}$  was attributed to one dipya ligand giving a mass loss of 68.55 % (calcd. 65.25 %), while up to the final temperature of the thermal degradation, another dipya ligand was lost. The detected mass of the solid residue of 22.73 % at  $850\text{ }^\circ\text{C}$  corresponds to the binary oxide  $2\text{CuO}\cdot\text{MnO}$ , which is in very good agreement with the calculated value of 22.62 %. A similar residue is observed after decomposition of  $[\text{Cu}_2\text{Mn(OAc)}_6(\text{bipy})_2]^{32}$  where

OAc<sup>-</sup> and bipy correspond to the acetate anion and 2,2'-bipyridine, respectively. Under a N<sub>2</sub> atmosphere, all processes are endothermic as expected.

#### *Magnetic properties of complex I*

The magnetic susceptibility of powdered sample **I** was measured in a magnetic field of 100 mT as a function of temperature in the range 2–300 K. The measured data were corrected for the temperature-independent Larmor diamagnetic susceptibility obtained from Pascal's tables<sup>33</sup> and for the sample holder contribution. Temperature variation of magnetic susceptibility is shown in Fig. 6. The susceptibility  $\chi(T)$  monotonically increases with decreasing temperature while the product  $\chi T$  changes only slightly from  $80 \times 10^6 \text{ m}^3 \text{ K mol}^{-1}$  at 300 K to a minimal value of  $60 \times 10^6 \text{ m}^3 \text{ K mol}^{-1}$  at 7 K indicating prevailing paramagnetic behavior of **I**. The fit of  $\chi$  vs.  $T$  data for  $T > 40$  K with the Curie–Weiss Law (full line in Fig. 6) gives the Curie constant  $C = 80 \times 10^6 \text{ m}^3 \text{ K mol}^{-1}$  and the Curie–Weiss temperature  $\theta = -4.7$  K. Three ions contribute to the total Curie constant  $C$ : one Mn<sup>2+</sup> and two Cu<sup>2+</sup>. If the orbital angular momentum of all ions is considered to be completely quenched ( $S = 5/2$ ,  $\mu_{\text{eff}} = 5.92 \mu_B$  for Mn<sup>2+</sup>, and  $S = 1/2$ ,  $\mu_{\text{eff}} = 1.73 \mu_B$  for Cu<sup>2+</sup>),<sup>34,35</sup> the total Curie constant should be  $65 \times 10^6 \text{ m}^3 \text{ K mol}^{-1}$ . As the measured Curie constant is larger than the theoretically expected, and there is no indication of ferromagnetic interaction effective at high temperatures, it could be concluded the orbital angular momentum  $L$  is not completely quenched.

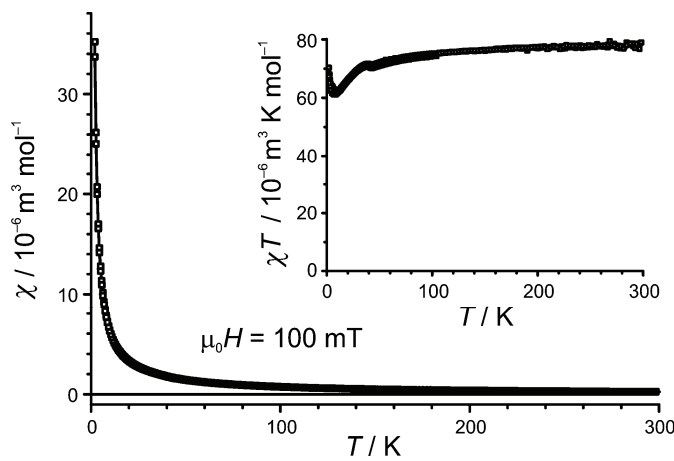


Fig. 6. The temperature dependence of the magnetic susceptibility of **I** in the form of  $\chi$  vs.  $T$  and the product  $\chi T$  vs.  $T$  (inset).

The obtained negative Curie–Weiss temperature  $\theta = -4.7$  K could, in principle be due to an antiferromagnetic interaction between metal ions and/or the effect of a spin–orbit coupling. As no maximum was observed in the  $\chi(T)$  dependence that is usually a result of considerable antiferromagnetic interaction, and

the non-zero contribution of the orbital angular momentum  $\mathbf{L}$  has already been shown, the negative  $\theta$  is very probably the effect of a spin–orbit coupling. The obtained  $\theta$  value thus could be understood only as an additional fitting parameter that improves the fit and tries to describe a smooth temperature dependence of the product  $\chi T$  between 300 and 40 K due to the  $\mathbf{L}$ – $\mathbf{S}$  coupling rather than an indication of antiferromagnetic interaction. A weak upturn of the product  $\chi T$  vs.  $T$  below 7 K might be an indication of a minor ferromagnetic interaction between the magnetic ions.

The isothermal magnetization curve  $M(H)$  measured at a temperature of 5 K is shown in Fig. 7. The full line in Fig. 7 is a function that is the sum of two Brillouin functions: the one with a total spin  $\mathbf{J} = 5/2$  for  $\text{Mn}^{2+}$  and the second one with  $\mathbf{J} = 1/2$  and double amplitude accounting for the two  $\text{Cu}^{2+}$ . Excellent correspondence between the function and the measured data is an additional confirmation of negligible interaction between magnetic ions in **I**.

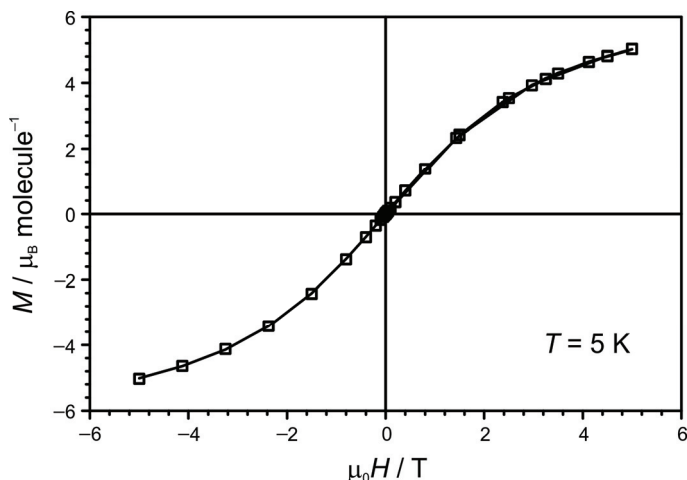


Fig. 7. Isothermal magnetization  $M(H)$  at 5 K of **I**. Full line is a function which is the sum of two Brillouin functions as described in the text.

## CONCLUSIONS

This study considered the synthesis, crystal structure, and the spectral, thermal and magnetic properties of a bimetallic Cu(II)–Mn(II) complex with bridging tpht and terminal dipya ligands, with the formulae  $[\text{Cu}_2\text{Mn}(\text{dipya})_2(\text{tpht})_3]_n$ , **I**. Due to the existence of two crystallographically different tpht ligands, the crystal packing of **I** is comprised of polymeric layers extending along the *ab*-plane. The geometry of Cu(II) and Mn(II) atoms can be described as octahedral, whereby the octahedron around the Cu(II) is very distorted because of the Jahn–Teller effect. The three-dimensional structure of **I** is achieved by intermolecular hydrogen bonds between the polymeric layers, which are further stabilized by

C–H $\cdots\pi$  interactions. Complex **I** is thermally stable up to 230 °C. Complete thermal degradation resulted in the mixed oxide 2CuO·MnO. Regarding the magnetic susceptibility measurements, complex **I** was found to exhibit paramagnetic behavior, with calculated  $C$  and  $\theta$  values of  $80 \times 10^6$  m $^3$  K mol $^{-1}$  and –4.7 K, respectively, whereby the latter results from spin–orbit coupling.

#### SUPPLEMENTARY MATERIAL

CCDC No. 1528723 contains the supplementary crystallographic data for this paper. These data can be obtained free of charge via <http://www.ccdc.cam.ac.uk/conts/retrieving.html>, or from the Cambridge Crystallographic Data Centre, 12 Union Road, Cambridge CB2 1EZ, UK; fax: (+44) 1223-336-033; or e-mail: deposit@ccdc.cam.ac.uk.

*Acknowledgements.* The authors gratefully acknowledge financial support from the Ministry of Education, Science and Technological Development of the Republic of Serbia (Grant No. III45007) and from the Slovenian Research Agency (Grant No. P2-0348).

ИЗВОД  
ХЕТЕРОНУКЛЕАРНИ ДВОДИМЕНЗИОНАЛНИ CU(II)–MН(II) КОМПЛЕКС СА  
МОСТОВНИМ ТЕРЕФТАЛАТ-ЛИГАНДИМА И ТЕРМИНАЛНИМ  
2,2'-ДИПРИДИЛАМИН- ЛИГАНДОМ

ЛИДИЈА РАДОВАНОВИЋ<sup>1</sup>, ЈЕЛЕНА РОГАН<sup>2</sup>, ДЕЈАН ПОЛЕТИЋ<sup>2</sup>, МАРКО В. РОДИЋ<sup>3</sup> и ЗВОНКО ЈАГЛИЧИЋ<sup>4</sup>

<sup>1</sup>Иновациони центар Технолошко–мешавинске факултета, Универзитет у Београду, Карнеијева 4,  
11000 Београд, <sup>2</sup>Технолошко–мешавински факултет, Универзитет у Београду, Карнеијева 4, 11000  
Београд, <sup>3</sup>Природно–математички факултет, Три Доситеја Обрадовића 3, 21000 Нови Сад и <sup>4</sup>Faculty  
of Civil and Geodetic Engineering & Institute of Mathematics, Physics and Mechanics, University of  
Ljubljana, Jamova 2, 1000 Ljubljana, Slovenia

Хетеронуклеарни Cu(II)–Mn(II) комплекс са мостовним терефталат-лигандима [Cu<sub>2</sub>Mn(dipy)<sub>2</sub>(tpht)<sub>3</sub>]<sub>n</sub>, **I**, где dipyра одговара 2,2'-дипридилиамину, а tpht је анјон 1,4-бензендикарбоксилне (терефталне, H<sub>2</sub>tpht) киселине, синтетисан је хидротермалном методом. Добијени комплекс **I** окарактерисан је рендгенском структурном анализом, FTIR спектроскопијом, TG/DSC анализом и мерењем магнетне сусцептивности. Cu(II) и Mn(II) метални центри налазе се у деформисаном октаедарском окружењу и повезани су мостовним tpht-лигандима. Два кристалографски различита tpht-анјона координирана су као тридентатни и хексадентатни лиганди и формирају дводимензионалне слојеве. Слојеви су повезани водоничним везама и додатно стабилизовани нековалентним C–H $\cdots\pi$  интеракцијама. Мерења магнетне сусцептивности показала су да је **I** скоро савршени парамагнет.

(Примљено 25. априла, ревидирано 8. јуна, прихваћено 7. јула 2017)

#### REFERENCES

1. a) P. Buchwalter, J. Rosé, P. Braunstein, *Chem. Rev.* **115** (2015) 28; b) L. J. Murray, M. Dincă, J. R. Long, *Chem. Soc. Rev.* **38** (2009) 1294; c) Y. Q. Sun, Y. Y. Xu, L. Wu, Y. F. Zheng, D. Z. Gao, G. Y. Zhang, *Polyhedron* **91** (2015) 1
2. X. J. Kong, Y. P. Ren, W. X. Chen, L. S. Long, Z. Zheng, R. B. Huang, L. S. Zheng, *Angew. Chem., Int. Ed.* **47** (2008) 2398
3. S. X. Cui, Y. L. Zhao, J. P. Zhang, Q. Liu, *J. Mol. Struct.* **927** (2009) 21
4. a) X. S. Tan, J. Sun, D. F. Xiang, W. X. Tang, *Inorg. Chim. Acta* **255** (1997) 157; b) L. C. Francesconi, D. R. Corbin, A. W. Clauss, D. N. Hendrickson, G. D. Stucky, *Inorg. Chem.* **20** (1981) 2078

5. C. E. Xanthopoulos, M. P. Sigalas, G. A. Katsoulos, C. A. Tsipis, A. Terzis, M. Mentzasos, A. Hountas, *Inorg. Chem.* **32** (1993) 5433
6. Y. Z. Zheng, Z. Zheng, X. M. Chen, *Coord. Chem. Rev.* **258–259** (2014) 1
7. M. Kurmoo, *Chem. Soc. Rev.* **38** (2009) 1353
8. H. X. Zhang, B. S. Kang, A. W. Xu, Z. N. Chen, Z. Y. Zhou, A. S. C. Chan, K. B. Yuc, C. Ren, *J. Chem. Soc., Dalton Trans.* (2001) 2559
9. E. G. Bakalbassis, J. Mrozinski, C. A. Tsipis, *Inorg. Chem.* **24** (1985) 3548
10. L. Deakin, A. M. Arif, J. S. Miller, *Inorg. Chem.* **38** (1999) 5072
11. M. Kurmoo, H. Kumagai, M. A. Green, B. W. Lovett, S. J. Blundell, A. Ardavan, J. Singleton, *J. Solid State Chem.* **159** (2001) 343
12. J. Cano, G. De Munno, J. L. Sanz, R. Ruiz, J. Faus, F. Lloret, M. Julve, A. Caneschi, *J. Chem. Soc., Dalton Trans.* (1997) 1915
13. J. Cano, G. De Munno, J. Sanz, R. Ruiz, F. Lloret, J. Faus, M. Julve, *J. Chem. Soc., Dalton Trans.* (1994) 3465
14. D. Sun, R. Cao, Y. Liang, Q. Shi, W. Su, M. Hong, *J. Chem. Soc., Dalton Trans.* (2001) 2335
15. W. G. Lu, J. H. Deng, D. C. Zhong, *Inorg. Chem. Commun.* **20** (2012) 312
16. L. Radovanović, J. Rogan, D. Poleti, M. V. Rodić, N. Begović, *Inorg. Chim. Acta* **445** (2016) 46
17. D. Poleti, J. Rogan, M. V. Rodić, L. Radovanović, *Acta Crystallogr., C* **71** (2015) 110
18. Lj. Karanović, D. Poleti, J. Rogan, G. A. Bogdanović, A. Spasojević-de Biré, *Acta Crystallogr., C* **58** (2002) m275
19. L. Radovanović, J. Rogan, D. Poleti, M. Milutinović, M. V. Rodić, *Polyhedron* **112** (2016) 18
20. Y. B. Go, X. Wang, E. V. Anokhina, A. Jacobson, *Inorg. Chem.* **44** (2005) 8265
21. C. R. Groom, F. H. Allen, *Angew. Chem., Int. Ed.* **53** (2014) 662
22. H. Hu, R. H. Zhang, F. Yang, Y. H. Zhang, Q. L. Wang, G. M. Yang, *Inorg. Chem. Commun.* **40** (2014) 87
23. M. C. Burla, C. Giacovazzo, G. Polidori, *J. Appl. Crystallogr.* **46** (2013) 1592
24. G. M. Sheldrick, *Acta Crystallogr., C* **71** (2015) 3
25. L. J. Farrugia, *J. Appl. Crystallogr.* **45** (2012) 849
26. M. A. Halceow, *Chem. Soc. Rev.* **42** (2013) 1784
27. a) N. E. Brese, M. O'Keeffe, *Acta Crystallogr., B* **47** (1991) 192; b) I. D. Brown, *The Chemical Bond in Inorganic Chemistry: The Bond Valence Model*, Oxford University Press, Oxford, 2002
28. E. G. Bakalbassis, J. Mrozinski, C. A. Tsipis, *Inorg. Chem.* **25** (1986) 3684
29. G. B. Deacon, R. J. Phillips, *Coord. Chem. Rev.* **33** (1980) 227
30. K. Nakamoto, *Applications in Coordination Chemistry*, in *Infrared and Raman Spectra of Inorganic and Organic Coordination Compounds*, Part B, 5<sup>th</sup> ed., K. Nakamoto, Wiley-Interscience, New York, 1997, p. 60 (for coordination modes of COO groups) and p. 55 (for M–O vibrations)
31. E. Castellucci, L. Angeloni, N. Neto, G. Sbrana, *Chem. Phys.* **43** (1979) 365
32. V. G. Makhankova, O. V. Khavryuchenko, V. V. Lisnyak, V. N. Kokozay, V. V. Dyakonenko, O. V. Shishkin, B. W. Skelton, J. Jezierska, *J. Solid State Chem.* **183** (2010) 2695
33. G. A. Bain, J. F. Berry, *J. Chem. Educ.* **85** (2008) 532
34. N. W. Ashcroft, N. D. Mermin, *Solid State Physics*, Saunders College Publishing, Philadelphia, PA, 1976
35. F. E. Mabbs, D. J. Machin, *Magnetism and Transition Metal Complexes*, Dover Publications, Inc. Mineola, New York, 1973.